Effect of mutations of N- and C-terminal charged residues on the activity of LCAT

Frank Peelman,* Berlinda Vanloo,* Jean-Luc Verschelde,[†] Christine Labeur,* Hans Caster,* Josée Taveirne,* Annick Verhee,[†] Nicolas Duverger,[§] Joël Vandekerckhove,[†] Jan Tavernier,[†] and Maryvonne Rosseneu[1],*

Laboratory for Lipoprotein Chemistry* and Department of Biochemistry,[†] Faculty of Medicine, Flanders Interuniversity Institute for Biotechnology, Universiteit Gent, B-9000 Ghent, Belgium; and Cardiovascular Department,[§] Aventis, 94403 Vitry sur Seine, France

Abstract On the basis of structural homology calculations, we previously showed that lecithin:cholesterol acyltransferase (LCAT), like lipases, belongs to the α/β hydrolase fold family. As there is higher sequence conservation in the N-terminal region of LCAT, we investigated the contribution of the N- and C-terminal conserved basic residues to the catalytic activity of this enzyme. Most basic, and some acidic residues, conserved among LCAT proteins from different species, were mutated in the N-terminal (residues 1–210) and C-terminal (residues 211–416) regions of LCAT. Measurements of LCAT-specific activity on a monomeric substrate, on low density lipoprotein (LDL), and on reconstituted high density lipoprotein (rHDL) showed that mutations of N-terminal conserved basic residues affect LCAT activity more than those in the C-terminal region. This agrees with the highest conservation of the α/β hydrolase fold and structural homology with pancreatic lipase observed for the N-terminal region, and with the location of most of the natural mutants reported for human LCAT. The structural homology between LCAT and pancreatic lipase further suggests that residues R80, R147, and D145 of LCAT might correspond to residues R37, K107, and D105 of pancreatic lipase, which form the salt bridges D105-K107 and D105-R37. ⬛ Natural and engineered mutations at residues R80, D145, and R147 of LCAT are accompanied by a substantial decrease or loss of activity, suggesting that salt bridges between these residues might contribute to the structural stability of the enzyme. —Peelman, F., B. Vanloo, J-L. Verschelde, C. Labeur, H. Caster, J. Taveirne, A. Verhee, N. Duverger, J. Vandekerckhove, J. Tavernier, and M. Rosseneu. **Effect of mutations of N- and C-terminal charged residues on the activity of LCAT.** *J. Lipid Res.* 2001. **42:** 471–479.

Supplementary key words enzyme • lipase • structure • ionic interactions • phospholipid • lipoproteins

Lecithin:cholesterol acyltransferase (LCAT) accounts for the synthesis of most of the plasma cholesteryl esters, thus participating in lipid metabolism (1). The enzyme has both a phospholipase A_2 and an acyl transferase activity, as it catalyzes the transacylation of the *sn*-2 fatty acid of lecithin to the free 3-β hydroxyl group of cholesterol whereby lysolecithin and cholesteryl esters are formed (2). LCAT is active both on low density lipoprotein (LDL) and high density lipoprotein (HDL), and several mutations in the LCAT gene lead to impaired enzymatic activity (3). Mutations causing familial LCAT deficiency (FLD) result in loss of activity on both lipoprotein substrates, whereas mutations causing fish-eye disease (FED) are associated with partial loss of activity on HDL only (3).

Using structural homology calculations based on threading methods, we proposed that LCAT, like lipases, belongs to the α/β hydrolase fold family, and we could identify conserved structural elements and variable loops in this protein (4, 5). The aligned sequences of human, baboon, rabbit, mouse, rat, chicken, and *Caenorhabditis elegans* LCAT show a homology profile with maximal residue conservation in the β strands and α helices (5). As a whole, the N-terminal part of the LCAT sequence (residues 1–210) is better conserved than the C-terminal domain (residues 211–416), because of the variability of the long excursion at residues 211–332 (4). We built a three-dimensional model for LCAT, using human pancreatic and *Candida antarctica* lipases as templates. This model consists of a central β sheet made of seven conserved β strands, sandwiched between two layers of two α helices (4). A long excursion at residues 211–332 separates the N- and C-terminal regions that form the α/β hydrolase core of LCAT. Using site-directed mutagenesis, we showed that, besides the S181 residue (6), the catalytic triad of LCAT includes D345 and H377, and identified the oxyanion hole resi-

dues F103 and L182. An interfacial recognition domain contributing to the enzyme-substrate interaction was proposed at residues 50–74 (7, 8), in which W61 plays a crucial role (7). The three-dimensional model of LCAT provided a structural interpretation for the effects of natural point mutations in the LCAT gene, accounting for the decreased LCAT activity on HDL, LDL, or on both substrates (5, 9). We showed that decreased acyltransferase activity on HDL, characteristic for FED mutants, is due to decreased phospholipase A_2 activity, whereas esterase activity on a monomeric substrate is retained (9). These results demonstrated that residues T123 and F382 of LCAT contribute to enzyme activation by the apolipoprotein A-I (apoA-I) cofactor (9).

Besides the homology between secondary structure elements, sequence homology was observed between residues of conserved β strands and α helices in LCAT and in several lipases (4, 10). The core of LCAT and lipases consists of a central β sheet, sandwiched between two layers of helices. The structure is stabilized both by hydrophobic interactions and by salt bridges, as described for the fungal lipase and the type B carboxylesterase families (11–13). To investigate the contribution of conserved charged residues in the N- and C-terminal regions of LCAT to the catalytic activity, most basic and some acidic conserved residues were mutated. The mutant proteins were expressed in COS-1 cells, esterase activity was measured on a monomeric substrate, and acyltransferase activity was assayed both on LDL and on reconstituted HDL (rHDL). The activity measurements of the in vitro mutants are consistent with the sequence conservation between LCAT species, the structural homology between LCAT and other lipolytic enzymes, and with the location of most of the natural mutations identified in human LCAT.

MATERIALS AND METHODS

Sequence alignments and analysis of sequence conservation

Remote sequence homologs of human LCAT were detected and aligned, using the hidden Markov model method SAM-T99, available at: http://www.cse.ucsc.edu/research/compbio/HMM-apps/HMM-applications.html (14, 15). The SAM-T99 method was also applied to detect structural homology between human LCAT and protein structures in the SCOP (Structural Classification of Proteins) and PDB (Protein Data Bank) databases. The SAM-T99 sequence alignment of the best conserved LCAT homologs were plotted by ALSCRIPT, and the conservation index per residue was calculated by the AMAS program available at http://barton.ebi.ac.uk/servers/amas_server.html (16, 17).

The distribution of charged residues in human LCAT and the average residue conservation were calculated by moving a 21-residue window along the sequence. The average charge value and mean conservation index were plotted as a function of the central residue of the window. The three-dimensional model for LCAT was built with HOMOLOGY software (MSI, San Diego, CA).

Site-directed mutagenesis and transient expression of LCAT mutants in COS-1 cells

Mutagenesis was carried out in the pXL 3105 plasmid vector (4), using the Quick Change site-directed mutagenesis method (Stratagene, La Jolla, CA). Mutations were built in by polymerase chain reaction, using *PfU* DNA polymerase. After *Dpn*I digestion of the parental Dam-methylated template, the synthesized mutated DNA was transformed into *Escherichia coli* XL1-Blue supercompetent cells. Colonies were screened by restriction analysis and mutants were sequenced on an ALF automated sequencer (Pharmacia Biotech, Piscataway, NJ). Transient expression of the LCAT cDNA in COS-1 cells was carried out by LipofectAMINE (GIBCO, Grand Island, NY) transfection. After transfection, the cell culture media (Dulbecco's modified Eagle's medium; Life Technologies, Rockville, MD) were changed to Opti-MEM after 16 h, and media containing the secreted LCAT enzyme were collected after 48 h.

Measurement of LCAT activity and concentration

The activity of wild-type LCAT and mutants was measured on three different substrates: rHDL, LDL, and a monomeric phospholipid analogue. rHDL, consisting of 1-palmitoyl-2-linoleoylphosphatidylcholine, cholesterol, and apoA-I at a molar ratio of 100:10:1, was prepared by the cholate-dialysis method (18). The percentage of cholesteryl esters formed after 30 min of incubation with LCAT was assayed by high performance liquid chromatography (HPLC) (19, 20). LDL was purified from plasma by sequential ultracentrifugation, heat inactivated at 56°C, and labeled with [^{3}H]cholesterol (21). After incubation of 350 µl of cell culture medium, containing 500–700 ng of secreted LCAT, with LDL for 3 h, lipids were extracted with 4 ml of hexane–isopropanol 3:2 (v/v). Unesterified cholesterol and cholesteryl esters were separated by thin-layer chromatography on silica gel plates developed in hexane–diethyl ether–acetic acid 90:20:1 (v/v/v) and quantified by liquid scintillation (21). The esterase activity of LCAT was measured on monomeric 1,2-bis-(1-pyrenebutanoyl)-*sn*-glycero-3-phosphocholine by HPLC (7, 22). The assay mixture contained 1 µM 1,2-bis-(1-pyrenebutanoyl)-*sn*-glycero-3-phosphocholine, 4 mM 2-mercaptoethanol, and bovine serum albumin (4 mg/ml), to which 350 µl of cell culture medium containing 500–700 ng of secreted LCAT, and 10 mM Tris-HCl buffer, pH 8.0, containing 0.15 M NaCl, 3 mM ethylenediaminetetraacetic acid, and 1 mM NaN_3, were added to a final volume of 0.5 ml. After incubation at 37°C for 10 min, the reaction was stopped by addition of 4 ml of chloroform–methanol 2:1 (v/v) containing 1-pyrenehexanoic acid as internal standard. 1-Pyrenebutanoic acid was quantified by isocratic HPLC (600E; Waters, Milford, MA) on a reversed-phase ODS C_{18} column (Licrocart 2504; Merck, Rahway, NJ), eluted with acetonitrile–water–trifluoroacetic acid 70:30:0.1 (v/v/v), and detected at 342 nm. LCAT concentration was measured by solid-phase enzyme immunoassay, using chicken antibodies specific to human LCAT. Purified recombinant human LCAT, produced in a stable baby hamster kidney cell line, was used as a standard (4). All enzymatic activities were expressed as specific activities, which were comparable for LCAT purified from human plasma and for wild-type LCAT secreted in the COS-1 medium. The activities of the mutants were expressed as percentages of wild-type LCAT activity.

RESULTS

Identification of the conserved charged residues in LCAT

Results of a structural homology search between LCAT and the SCOP and PDB structure databases, using the hidden Markov model method SAM-T99, indicated that LCAT belongs to the α/β hydrolase family, as previously detected by using threading algorithms (4). A remote se-

quence homology search with SAM-T99 (14, 15) showed that LCAT belongs to a large esterase family, containing vertebrate, invertebrate, plant, bacteria, and fungi members. The SAM-T99 sequence alignment of human, baboon, rabbit, rat, mouse, and chicken LCAT; of the newly identified LCAT-like lysophospholipase (23) from human macrophages; of LCAT-like sequences of *Drosophila melanogaster* (GenBank AAD38574), *C. elegans* (CAA95833) (24), *Arabidopsis thaliana* (AAC80628, AAD10668), and *Schizosaccharomyces pombe* (CAA22887); of a hypothetical 75.4-kDa *Saccharomyces cerevisiae* protein (CAA54576) (25); and of the *Bacillus licheniformis* esterase (AAA79183) (26) is shown in **Fig. 1**. The positively charged residues in human LCAT, which are completely conserved in the LCAT sequences of the vertebrate species, are as follows: K39, K42, R52, K53, R80, R99, K105, K116, R135, R140, R147, K199, K218, K238, K240, R244, R280, and R298. Among these residues, only R147 is identical in all the aligned sequences shown in Fig. 1, whereas either R or K is present at position 240 (Fig. 1). R52 and K53 belong to the putative interfacial recognition domain of LCAT (7, 8), residues R80 and R147 follow the conserved strands β2 and β4, respectively, and R99 belongs to the predicted strand β3. The conserved lysine or arginine residues K238, K240, R244, K280, and R298 are located on the long excursion between strands 6 and 7. R351, which is conserved in five vertebrate LCAT sequences, is part of the loop between strands β7 and β8 in the three-dimensional LCAT model (4). The fully conserved negatively charged residues in the LCAT sequences of the vertebrate species are as follows: E37, D41, E55, D73, D77, E110, D113, D136, D145, E155, E165, E166, D200, D227, E241, E242, E261, D262, D277, D284, E288, E289, D299, D328, D335, D343, D345, D346, and E354. Among these residues, only D145 and the catalytic triad residue D345 remain identical in all sequences listed in Fig. 1, whereas an acidic residue is conserved at position 165.

Figure 1 shows the sequence conservation between LCAT from different species and related proteins of the α/β hydrolase family. Secondary structure elements in human LCAT are shown in Fig. 1. Several gaps are observed in the sequence alignment, for example, at residue 115 in the N-terminal part of the protein, because of long inserts in the more divergent sequences. **Figure 2** shows the conservation index for all residues and the mean protein charge along the sequence, averaged over a 21-residue window. LCAT is predominantly negatively charged, with charge minima around residues 70, 140, and 345. A smaller net positive charge was calculated around residues 95, 180, and 240. The sequence conservation index was considered significant above a threshold value of 4 (17). It is maximal between residues 110 and 250, including the catalytic residue S181, and between residues 320 and 350, including the catalytic triad residue D345. Most point mutations associated with either FLD or FED were identified in those regions in human LCAT (Fig. 2) (3, 5, 27). The relative frequency of point mutations in the conserved regions between residues 110 and 250, and between residues 320 and 350, of LCAT is 12/170 residues (7%) for the most severe FLD mutations and 3/170 (2%) for the FED muta-

tions, respectively. In the N- and C-terminal parts of the sequence, there are eight FLD and three FED mutations, corresponding to respective frequencies of 3 and 1.5%.
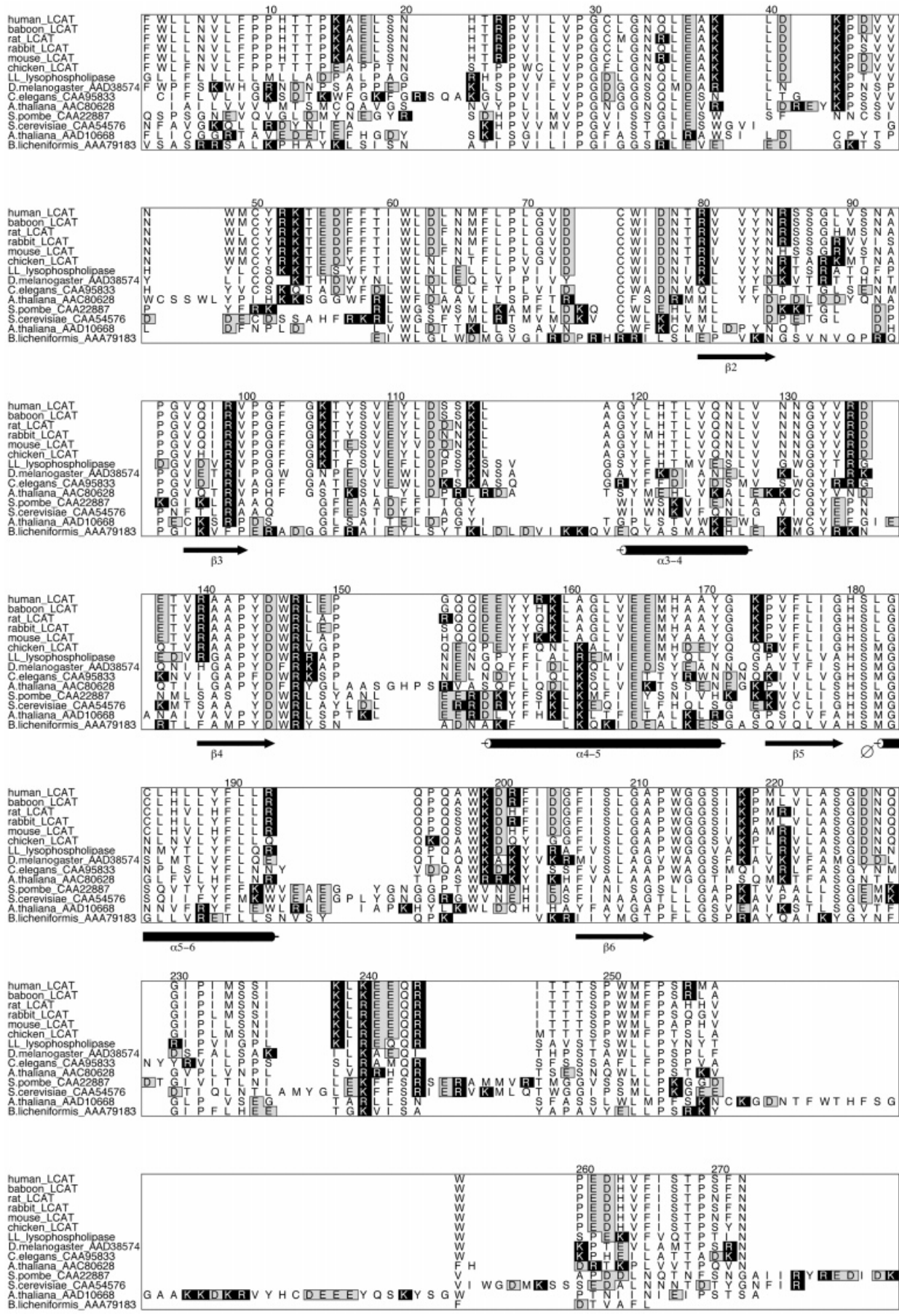
The three-dimensional model for LCAT, built from the crystal structures of pancreatic lipase and *C. antarctica* lipase, is shown in **Fig. 3**. Residues 100–210 and 332–416 constitute the core of the LCAT α/β hydrolase model structure, and a long loop at residues 211–332 separates the N- from the C-terminal region. We mutated the conserved charged residues in the N-terminal (1–210) and C-terminal regions (211–416) of LCAT, and measured the activity of the mutants on different substrates.

Effect of mutations of conserved charged residues in the N-terminal region of LCAT on catalytic activity

The mutants were expressed at concentrations ranging between 0.6 and 2.1 μg/ml, that is, between 30% and 100% of wild-type LCAT, with the exception of mutant K39A, which was not expressed as the construct could not be generated in *E. coli* (**Table 1**). Among the conserved N-terminal basic residues, the K42A mutant lost activity on both HDL and LDL, while retaining 10% activity on a monomeric substrate. Residues R52 and K53 were postulated to belong to an interfacial recognition domain or lid in LCAT (7, 8). The lid is closed by a disulfide bridge between C50 and C74, and might cover the catalytic cavity of the enzyme. As expected, single mutations at positions 52 and 53 decrease LCAT activity on the organized HDL and LDL substrates, while retaining activity on a monomeric substrate (Table 1). The double mutation R52A/K53A impaired almost completely the activity on all substrates. The R80Q mutant lost about 40% activity on the monomeric substrate, and about 60% activity on LDL and rHDL (Table 1). The R99Q mutant retained about 60% activity on all substrates, whereas a natural R99C mutation at this position induces an FED phenotype (28).

The next arginine residues, R135, R140, and R147, are critical for LCAT activity, as arginine-alanine mutations at these positions abolished the catalytic activity on all substrates (Table 1). This is in agreement with the reported natural mutations R135W, R140H, and R147W, associated with FLD (3, 29). When the natural R147W mutant was expressed in COS-1 cells, its activity was decreased on all substrates (Table 1). Mutation of acidic residues E110Q, D113N, and D145N abolished LCAT activity on all substrates (Table 1), whereas the D136N mutation decreased LCAT activity on LDL by only 50%. In this region, D145 and R147 are the only fully conserved residues in all proteins of the LCAT family listed in Fig. 1. Mutation of these residues completely abolishes activity on all substrates. Wang et al. (30) mutated residues E154, E155, and E165 to a lysine in helix α4–5 of LCAT, and concluded that these mutations do not significantly affect the enzymatic activity. Although an acidic residue is conserved at position 165 in all species listed in Fig. 1, this negative charge does not seem critical for enzymatic activity.

Threading alignments showed that residues R80, R147, and D145 in human LCAT align with R37, K107, and D105 in pancreatic lipase. Within the lipase family, align-

Fig. 1. Multiple sequence alignments of human, baboon, rabbit, rat, mouse, and chicken lecithin:cholesterol acyltransferase (LCAT); of the newly identified LCAT-like lysophospholipase from human THP-1 macrophages; of the LCAT-like sequences of *Drosophila melanogaster* (GenBank AAD38574), *Caenorhabditis elegans* (CAA95833), *Arabidopsis thaliana* (AAC80628, AAD10668), and *Schizosaccharomyces pombe* (CAA22887); of the hypothetical 75.4-kDa *Saccharomyces cerevisiae* protein; and of the *Bacillus licheniformis* esterase (AAA79183). Predicted α helices and β strands (4) and active site residues (open triangles) are indicated under the alignment. Black, positively charged residues K or R; gray, negatively charged residues D or E.
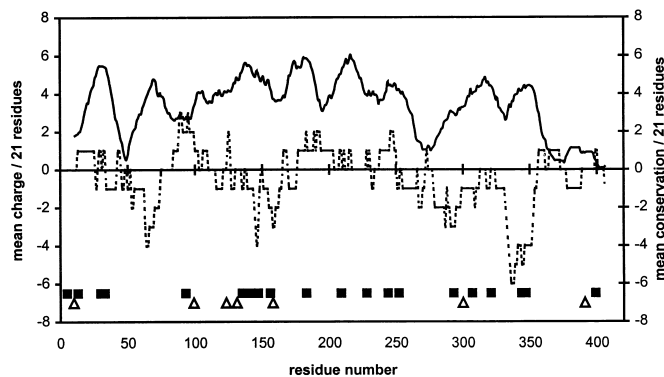
Fig. 2. Conservation index, calculated by AMAS (17) (solid line, right *y*-axis), and mean protein charge (dotted line, left *y*-axis), both averaged over a 21-residue window along the human LCAT sequence. The parameters are plotted as a function of the central residue of the window. Locations of the natural point mutations associated with either familial LCAT deficiency (FLD) (solid squares) or fish-eye disease (FED) (open triangles) are shown.

Fig. 3. Structural model of human LCAT, built on the basis of the crystalline structures of pancreatic lipase and *Candida antarctica* lipase as a template (4). Catalytic residues S181, D345, and H377 and possible salt bridge residues R80, D145, and R147 are indicated.

ment of residues 75–188 of LCAT with human pancreatic, hepatic, and lipoprotein lipases, and with the pancreatic lipase-related proteins PLRP-1 and PLRP-2, shows strict conservation (**Fig. 4**) (31). In the crystal structure of pancreatic lipase, R37 lies on strand β1 (21, 32, 33), whereas residues D105 and K107 follow strand β4 (Fig. 3). Residues R37 and K107 form a salt bridge with D105. Using the coordinates of Egloff et al. (34), the distances between N and O atoms are 4.5 and 3.5 Å for the ion pairs R37-D105 and K107-D105, respectively.
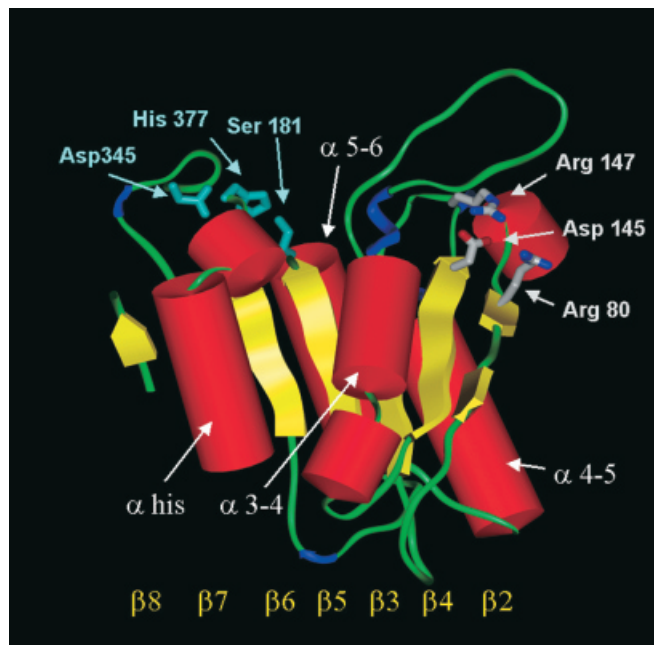
The structural homology between LCAT and pancreatic lipase (4) suggests that in LCAT, residues R80 and R147 might likewise form salt bridges with D145. This hypothesis is supported by the decreased activity of the engi-

TABLE 1. LCAT mass and relative specific activity in cell media from mutant and wild-type transfectants (n = 3)

Transfectant	Mass[a]	Acyltransferase Activity[a]		Esterase Activity[a]
		rHDL	LDL	
	μg/ml	*% wild type*		*% wild type*
Wild type	2.1 ± 0.5	100	100	100
K42A	1.9 ± 0.5	<1	<2	13 ± 5
K39A/K42A	2.1 ± 0.5	<1	<2	<1
R52A	1.3 ± 0.4	39 ± 10	34 ± 6	100 ± 10
K53A	2.5 ± 0.6	78 ± 15	32 ± 8	104 ± 15
R52A/K53A	1.5 ± 0.3	10 ± 5	<2	<1
R80Q	2.1 ± 0.5	46 ± 10	30 ± 7	67 ± 12
R99Q	2.0 ± 0.3	60 ± 15	61 ± 12	62 ± 13
E110Q	0.7 ± 0.2	<1	<2	<1
D113N	1.6 ± 0.3	<1	<2	<1
R135A	1.5 ± 0.3	<1	<1	<1
D136N	1.6 ± 0.4	127 ± 20	48 ± 10	108 ± 20
R140A	1.8 ± 0.3	<1	<1	<1
D145N	0.6 ± 0.2	<1	<2	<1
R147W	0.6 ± 0.1	<1	<2	<1
R147A	0.7 ± 0.2	<1	<2	<1
K238A/K240A	1.6 ± 0.3	68 ± 16	29 ± 6	39 ± 8
R280A	1.4 ± 0.4	84 ± 20	130 ± 18	70 ± 15
R298A	1.7 ± 0.5	47 ± 10	116 ± 20	120 ± 15
R351A	1.7 ± 0.4	72 ± 15	105 ± 20	64 ± 10

Acyltransferase activity was measured on rHDL and LDL. Esterase activity was measured on monomeric 1,2-bis(1-pyrene-butanoyl)-*sn*-glycero-3-phosphocholine as described. LCAT, lecithin:cholesterol acyltransferase; rHDL, reconstituted high density lipoprotein consisting of 1-palmitoyl-2-linoleoylphosphatidylcholine/cholesterol/apoA-I complexes at a molar ratio of 100:10:1; LDL, low density lipoprotein.

[a] Values are given ± SD.

```
PLRP1  33 EKI GTR FLLYTNEN--PNNFQILLLSDPSTIEASNFQMDRKTRFI IHGF -ID-------- 81
PLRP2  33 EDI DTR FLLYTNEN--PNNFQLITGTEPDTIEASNFQLDRKTRFI IHGF -LD-------- 81
HL     24 HEM KTR FLLFGETN---QGCQIRIN-HPDTLQECGFNSSLPLVMI IHGW SVD-------- 71
LPL     8 IDI ESK FALRTPEDTAEDTCHLIPG-VAESVATCHFNHSSKTFMV IHGW TVT-------- 58
PL     33 KDV NTR FLLYTNEN--PNNFQEVAA-DSSSISGSNFKTNRKTRFI IHGF -ID-------- 80
LCAT   75 WID NTR VVYNRSSG-------------------LVSNAPGVQIR VPGF -GKTYSVEYLD 113
              ↑  β2                                       β3

PLRP1  82 -KGDESWVTDMCKKLFE--V-----EE-VNCIC VDWK KGSQATYTQAANNVRVVGAQVAQ 132
PLRP2  82 -KAEDSWPSDMCKKMFE--V-----EK-VNCIC VDWR HGSRAMYTQAVQNIRVVGAETAF 132
HL     72 -GVLENWIWQMVAALKSQPA-----QP-VNVGL VDWI TLAHDHYTIAVRNTRLVGKEVAA 124
LPL    59 -GMYESWVPKLVAALYK--R-----EPDSNVIV VDWL SRAQEHYPVSAGYTKLVGQDVAR 110
PL     81 -KGEENWLANVCKNLFK--V-----ES-VNCIC VDWK GGSRTGYTQASQNIRIVGAEVAY 131
LCAT  114 SSKLAGYLHTLVQNLVN--NGYVRDET-VRAAP YDWR LEPGQQ--------ESYYRKLAG 164
                 α 3-4          β4    ↑↑            α 4-5

PLRP1 133 MLDILLTEYSYPPSK VHLIGHSLG AHVAG 161
PLRP2 133 LIQALSTQLGYSLED VHVIGHSLG AHTAA 161
HL    125 LLRWLEESVQLSRSH VHLIGYSLG AHVSG 153
LPL   111 FINWMEEEFNYPLDN VHLLGYSLG AHAAG 139
PL    132 FVEFLQSAFGYSPSN VHVIGHSLG AHAAG 160
LCAT  165 LVEEMHAAYG---KP VFLIGHSLG CLHLL 188
              α 4-5           β5
```

Fig. 4. Multiple sequence alignment of the human pancreatic lipase-related proteins PLRP-1 and PLRP-2, human hepatic lipase (HL), lipoprotein lipase (LPL), and pancreatic lipase (PL) with human LCAT (residues 75–188). Homologous residues in lipases and LCAT are boxed and structural elements predicted in LCAT are underlined. Residues that form salt bridges in pancreatic lipase and corresponding residues in LCAT are indicated by arrows.

neered mutant R80Q, the loss of activity of the D145N, R147A, and R147W mutants, and by the natural mutation R147W, associated with FLD (3, 29). Whereas D145 and R147 are strictly conserved in all members of the LCAT family, R80 is conserved only in the closest LCAT homologs, suggesting weaker homology (Fig. 1). The structural homology between R37 in pancreatic lipase and R80 in LCAT is also weaker than for the other residues, as R37 is located at the end of the extra N-terminal strand β1 in pancreatic lipase. This might account for the higher residual activity of the R80Q mutant.

Effect of mutations of conserved C-terminal charged residues on LCAT catalytic activity

Mutations of basic residues in the C-terminal half of the LCAT sequence had a lesser effect on the enzymatic activity, as all mutants, including the double mutant K238A/K240A, retained at least 30% activity on monomeric and organized substrates (Table 1). The activity of the R298A mutant on HDL was decreased, as also observed for the natural Δ300 mutation, which is associated with FED (35). This observation suggests that this LCAT region might be involved in the interaction with HDL and with the apoA-I cofactor. The decreased activity of the R80Q, D136N, and K238A/K240A mutants on LDL might result from thermal instability during the 3-h incubation at 37°C. The activity of these mutants at 37°C decreased more rapidly than that of wild-type LCAT as a function of time (data not shown).

We previously showed that histidine residue mutants H263A and H368A, and acidic residue mutants D227N, D328N, D335N, D343N, and D346N, in the C-terminal half of the LCAT sequence retain activity on monomeric and lipoprotein substrates. The enzymatic activity was abolished only by mutagenesis of active site residues H377 and D345 (4). Mutations at residues between positions 220 and 331 occur on the long excursion between strands β6 and β7, whose length and structure are highly variable among different lipases. The lower degree of conservation of the long excursion might account for the less detrimental effect of mutations in this region (4). R351 lies on the loop between strands β7 and β8 and is only partially conserved. Truncation of the proline-rich C-terminal residues 399–416 did not impair LCAT activity (36, 37).

CONCLUSION

In this article, we investigated the distribution and conservation of charged residues in the LCAT sequence and tested their contribution to LCAT activity. Mutagenesis of positively charged residues R39/K42, R52/K53, R80, and R147 and of negatively charged residues E110, D113, and D145 in the N-terminal half of LCAT decreases the enzymatic activity, whereas mutations of basic residues in the C-terminal region are less deleterious. This is in agreement with the relative preponderance of natural point mutations linked to FLD and FED, in the N-terminal region of LCAT (Fig. 2).

We previously mutated negatively charged residues in the C-terminal part of LCAT, and found that only mutation of D345 led to an inactive enzyme, indicating that it is probably an active site residue (4). Figure 1 shows that D345 is the only negatively charged residue in the C-terminal half of the sequence that is completely conserved in all aligned sequences.

We showed that mutagenesis of R149, R153, or R160 in apoA-I impairs LCAT activation, and that these residues could form a positively charged cluster that interacts with LCAT (38). The involvement of positively charged residues in apoA-I in LCAT activation suggests a possible interaction with negatively charged residues in LCAT. Mutagenesis of negatively charged residues in LCAT should decrease the activity of LCAT on HDL. We (4) and Wang et al. (30) mutated several conserved negatively charged residues in LCAT: E110Q, D113N, D136N, D147N, E154Q, E155Q, E165Q, D227N, D328N, D335N, D343N, D345N, and D346N. None of these mutants specifically decreased LCAT activity on HDL, indicating that they probably do not interact with arginine residues in apoA-I. Only the E110Q, D113N, D147N, and D345A mutations abolished activity on all substrates.

In lipases, the central core of the enzymes is stabilized by hydrophobic interactions between apolar residues of the amphipathic α helices and the β strands of the central β sheet. Hydrophobic forces can also contribute to the interaction between the amphipathic helices at the surface of LCAT and lipid substrates, as observed with synthetic peptides and with apolipoprotein fragments (39, 40). Salt bridges between residues on β strands and on loops were described in the crystal structure of *Geotrichum candidum* lipase (11), and in structurally related proteins. In fungal lipases, salt bridges between charged residues on conserved β strands in the central β sheet of these enzymes can further contribute to structural stabilization (12).

Binding of lipolytic enzymes to a hydrophobic lipid surface is potentially denaturing, as hydrophobic residues of the enzyme core can be exposed to the lipid. Denaturation at a lipid interface might thus be prevented by buried salt bridges (12). On the basis of structural homology between LCAT and pancreatic lipase, we postulated that residues R80 and R147 of LCAT might form stabilizing salt bridges with D145. This was supported by site-directed mutagenesis and activity measurements of the engineered mutants. Ionic interactions between R80 and the acidic residue are probably weaker, as the R80Q mutant retained more residual activity. This is reflected in the conservation of these residues: both D145 and R147 are completely conserved in all family members in Fig. 1, whereas R80 is conserved only in the LCAT sequences of vertebrates. We had previously proposed that the loss of activity of the natural R147W FLD mutant might be due to impairment of a salt bridge between R147 and D145 (5). This hypothesis is in agreement with the loss of in vitro activity of the D145 and R147 mutants reported here and with the strict conservation of these residues in all sequences of the LCAT family. ▮▮

Manuscript received 4 May 2000 and in revised form 1 November 2000.

REFERENCES

1. Glomset, J. A. 1968. The plasma lecithin:cholesterol acyltransferase reaction. *J. Lipid Res.* **9:** 155–167.
2. Jonas, A. 1998. Regulation of lecithin cholesterol acyltransferase activity. *Prog. Lipid Res.* **37:** 209–234.
3. Kuivenhoven, J. A., H. Pritchard, J. Hill, J. Frohlich, G. Assmann, and J. Kastelein. 1997. The molecular pathology of lecithin:cholesterol acyltransferase (LCAT) deficiency syndromes. *J. Lipid Res.* **38:** 191–205.
4. Peelman, F., N. Vinaimont, A. Verhee, B. Vanloo, J. L. Verschelde, C. Labeur, M. S. Seguret, N. Duverger, G. Hutchinson, J. Vandekerckhove, J. Tavernier, and M. Rosseneu. 1998. A proposed architecture for lecithin cholesterol acyl transferase (LCAT): identification of the catalytic triad and molecular modeling. *Protein Sci.* **7:** 587–599.
5. Peelman, F., J. L. Verschelde, B. Vanloo, C. Ampe, C. Labeur, J. Tavernier, J. Vandekerckhove, and M. Rosseneu. 1999. Effects of natural mutations in lecithin:cholesterol acyltransferase on the enzyme structure and activity. *J. Lipid Res.* **40:** 59–69.
6. Francone, O. L., and C. J. Fielding. 1991. Structure-function relationships in human lecithin:cholesterol acyltransferase. Site-directed mutagenesis at serine residues 181 and 216. *Biochemistry.* **30:** 10074–10077.
7. Peelman, F., B. Vanloo, O. Perez-Mendez, A. Decout, J. L. Verschelde, C. Labeur, N. Vinaimont, A. Verhee, N. Duverger, R. Brasseur, J. Vandekerckhove, J. Tavernier, and M. Rosseneu. 1999. Characterization of functional residues in the interfacial recognition domain of lecithin cholesterol acyltransferase (LCAT). *Protein Eng.* **12:** 71–78.
8. Adimoolam, S., and A. Jonas. 1997. Identification of a domain of lecithin-cholesterol acyltransferase that is involved in interfacial recognition. *Biochem. Biophys. Res. Commun.* **232:** 783–787.
9. Vanloo, B., K. Deschuymere, F. Peelman, J. Taveirne, A. Verhee, C. Gouyette, C. Labeur, J. Vandekerckhove, J. Tavernier, and M. Rosseneu. 2000. Relationship between structure and biochemical phenotype of lecithin:cholesterol acyltransferase (LCAT) mutants causing fish-eye disease. *J. Lipid Res.* **41:** 752–761.
10. Hide, W. A., L. Chan, and W. H. Li. 1992. Structure and evolution of the lipase superfamily. *J. Lipid Res.* **33:** 167–178.
11. Schrag, J. D., and M. Cygler. 1993. 1.8 Å refined structure of the lipase from *Geotrichum candidum. J. Mol. Biol.* **230:** 575–591.
12. Derewenda, U., L. Swenson, R. Green, Y. Wei, G. G. Dodson, S.

Yamaguchi, M. J. Haas, and Z. S. Derewenda. 1994. An unusual buried polar cluster in a family of fungal lipases. *Nat. Struct. Biol.* **1:** 36–47.
13. Cygler, M., J. D. Schrag, J. L. Sussman, M. Harel, I. Silman, M. K. Gentry, and B. P. Doctor. 1993. Relationship between sequence conservation and three-dimensional structure in a large family of esterases, lipases, and related proteins. *Protein Sci.* **2:** 366–382.
14. Karplus, K., C. Barrett, M. Cline, M. Diekhans, L. Grate, and R. Hughey. 1999. Predicting protein structure using only sequence information. *Proteins.* **37(Suppl. 3):** 121–125.
15. Karplus, K., C. Barrett, and R. Hughey. 1998. Hidden Markov models for detecting remote protein homologies. *Bioinformatics.* **14:** 846–856.
16. Barton, G. J. 1993. ALSCRIPT: a tool to format multiple sequence alignments. *Protein Eng.* **6:** 37–40.
17. Livingstone, C. D., and G. J. Barton. 1993. Protein sequence alignments: a strategy for the hierarchical analysis of residue conservation. *Comput. Appl. Biosci.* **9:** 745–756.
18. Matz, C. E., and A. Jonas. 1982. Micellar complexes of human apolipoprotein A-I with phosphatidylcholines and cholesterol prepared from cholate-lipid dispersions. *J. Biol. Chem.* **257:** 4535–4540.
19. Vercaemst, R., A. Union, M. Rosseneu, I. De Craene, G. de Backer, and M. Kornitzer. 1989. Quantitation of plasma free cholesterol and cholesteryl esters by high performance liquid chromatography. Study of a normal population. *Atherosclerosis.* **78:** 245–250.
20. Vanloo, B., J. Taveirne, J. Baert, G. Lorent, L. Lins, J. M. Ruysschaert, and M. Rosseneu. 1992. LCAT activation properties of apo A-I CNBr fragments and conversion of discoidal complexes into spherical particles. *Biochim. Biophys. Acta.* **1128:** 258–266.
21. Stokke, K. T., and K. R. Norum. 1971. Determination of lecithin:cholesterol acyltransfer in human blood plasma. *Scand. J. Clin. Lab. Invest.* **27:** 21–27.
22. Bonelli, F. S., and A. Jonas. 1992. Continuous fluorescence assay for lecithin:cholesterol acyltransferase using a water-soluble phosphatidylcholine. *J. Lipid Res.* **33:** 1863–1869.
23. Taniyama, Y., S. Shibata, S. Kita, K. Horikoshi, H. Fuse, H. Shirafuji, Y. Sumino, and M. Fujino. 1999. Cloning and expression of a novel lysophospholipase which structurally resembles lecithin cholesterol acyltransferase. *Biochem. Biophys. Res. Commun.* **257:** 50–56.
24. Wilson, R., R. Ainscough, K. Anderson, C. Baynes, M. Berks, J. Bonfield, J. Burton, M. Connell, T. Copsey, J. Cooper, et al. 1994. 2.2 Mb of contiguous nucleotide sequence from chromosome III of *C. elegans. Nature.* **368:** 32–38.
25. Verhasselt, P., R. Aert, M. Voet, and G. Volckaert. 1994. Twelve open reading frames revealed in the 23.6 kb segment flanking the centromere on the *Saccharomyces cerevisiae* chromosome XIV right arm. *Yeast.* **10:** 1355–1361.
26. Alvarez-Macarie, E., V. Augier-Magro, and J. Baratti. 1999. Characterization of a thermostable esterase activity from the moderate thermophile *Bacillus licheniformis. Biosci. Biotechnol. Biochem.* **63:** 1865–1870.
27. Peelman, F., J. Vandekerckhove, and M. Rosseneu. 2000. Structure and function of lecithin cholesterol acyl transferase: new insights from structural predictions and animal models. *Curr. Opin. Lipidol.* **11:** 155–160.
28. Blanco-Vaca, F., S. J. Qu, C. Fiol, H. Z. Fan, Q. Pao, A. Marzal-Casacuberta, J. J. Albers, I. Hurtado, V. Gracia, X. Pinto, T. Marti, and H. J. Pownall. 1997. Molecular basis of fish-eye disease in a patient from Spain. Characterization of a novel mutation in the LCAT gene and lipid analysis of the cornea. *Arterioscler. Thromb. Vasc. Biol.* **17:** 1382–1391.
29. Taramelli, R., M. Pontoglio, G. Candiani, S. Ottolenghi, H. Dieplinger, A. Catapano, J. Albers, C. Vergani, and J. McLean. 1990. Lecithin cholesterol acyl transferase deficiency: molecular analysis of a mutated allele. *Hum. Genet.* **85:** 195–199.
30. Wang, J., J. A. DeLozier, A. K. Gebre, P. J. Dolphin, and J. S. Parks. 1998. Role of glutamic acid residues 154, 155, and 165 of lecithin:cholesterol acyltransferase in cholesterol esterification and phospholipase A2 activities. *J. Lipid Res.* **39:** 51–58.
31. Giller, T., P. Buchwald, D. Blum-Kaelin, and W. Hunziker. 1992. Two novel human pancreatic lipase related proteins, hPLRP1 and hPLRP2. Differences in colipase dependence and in lipase activity. *J. Biol. Chem.* **267:** 16509–16516.
32. Winkler, F. K., A. D'Arcy, and W. Hunziker. 1990. Structure of human pancreatic lipase. *Nature.* **343:** 771–774.
33. Ollis, D. L., E. Cheah, M. Cygler, B. Dijkstra, F. Frolow, S. M. Fran-

ken, M. Harel, S. J. Remington, I. Silman, J. Schrag. 1992. The alpha/beta hydrolase fold. *Protein Eng.* **5:** 197–211.

34. Egloff, M. P., F. Marguet, G. Buono, R. Verger, C. Cambillau, and H. van Tilbeurgh. 1995. The 2.46 Å resolution structure of the pancreatic lipase-colipase complex inhibited by a C11 alkyl phosphonate. *Biochemistry.* **34:** 2751–2762.
35. Klein, H. G., S. Santamarina-Fojo, N. Duverger, M. Clerc, M. F. Dumon, J. J. Albers, S. Marcovina, and H. B. Brewer, Jr. 1993. Fish eye syndrome: a molecular defect in the lecithin-cholesterol acyltransferase (LCAT) gene associated with normal alpha-LCAT-specific activity. Implications for classification and prognosis. *J. Clin. Invest.* **92:** 479–485.
36. Francone, O. L., L. Evangelista, and C. J. Fielding. 1996. Effects of carboxy-terminal truncation on human lecithin:cholesterol acyltransferase activity. *J. Lipid Res.* **37:** 1609–1615.
37. Lee, Y. P., S. Adimoolam, M. Liu, P. V. Subbaiah, K. Glenn, and A.

Jonas. 1997. Analysis of human lecithin-cholesterol acyltransferase activity by carboxyl-terminal truncation. *Biochim. Biophys. Acta.* **1344:** 250–261.
38. Roosbeek, S., B. Vanloo, N. Duverger, H. Caster, J. Breyne, I. De Beun, H. Patel, J. Vandekerckhove, C. Shoulders, M. Rosseneu, and F. Peelman. 2001. Mutation of three conserved arginine residues in apolipoprotein A-I suppresses activation of lecithin cholesterol acyltransferase, and supports the "belt" model for discoidal rHDL particles. *J. Lipid Res.* **42:** 31–40.
39. Buchko, G. W., W. D. Treleaven, S. J. Dunne, A. S. Tracey, and R. J. Cushley. 1998. Structural studies of a peptide activator of human lecithin-cholesterol acyltransferase. *J. Lipid Res.* **39:** 51–58.
40. Wang, G., G. K. Pierens, W. D. Treleaven, J. T. Sparrow, and R. J. Cushley. 1996. Conformations of human apolipoprotein E(263–286) and E(267–289) in aqueous solutions of sodium dodecyl sulfate by CD and ^{1}H NMR. *Biochemistry.* **35:** 10358–10366.